

# Near-Infrared Luminosity Function and Colours of Dwarf Galaxies in the Coma Cluster

Bahram Mobasher<sup>1</sup> & Neil Trentham<sup>2</sup>

<sup>1</sup>*Astrophysics Group, Blackett Laboratory, Imperial College, Prince Consort Rd, London SW7 2BZ, UK*

<sup>2</sup>*Institute for Astronomy, University of Hawaii, 2680 Woodlawn Drive, Honolulu HI 96822, U.S.A.*

15 May 2019

## ABSTRACT

We present  $K$ -band observations of the low-luminosity galaxies in the Coma cluster, which are responsible for the steep upturn in the optical luminosity function at  $M_R \sim -16$ , discovered recently. The main results of this study are

(i) The optical–near-infrared colours of these galaxies imply that they are dwarf spheroidal galaxies. The median  $B - K$  colour for galaxies with  $-19.3 < M_K < -16.3$  is 3.6 mag.

(ii) The  $K$ -band luminosity function in the Coma cluster is not well constrained, because of the uncertainties due to the field-to-field variance of the background. However, within the estimated large errors, this is consistent with the  $R$ -band luminosity function, shifted by  $\sim 3$  magnitudes.

(iii) Many of the cluster dwarfs lie in a region of the  $B - K$  vs.  $B - R$  colour-colour diagram where background galaxies are rare ( $B - K < 5$ ;  $1.2 < B - R < 1.6$ ). Local dwarf spheroidal galaxies lie in this region too. This suggests that a better measurement of the  $K$ -band cluster luminosity function can be made if the field-to-field variance of the background can be measured as a function of colour, even if it is large.

(iv) If we assume that none of the galaxies in the region of the  $B - K$  vs.  $B - R$  plane given in (iii) in our cluster fields are background, and that all the cluster galaxies with  $15.5 < K < 18.5$  lie in this region of the plane, then we measure  $\alpha = -1.41^{+0.34}_{-0.37}$  for  $-19.3 < M_K < -16.3$ , where  $\alpha$  is the logarithmic slope of the luminosity function. The uncertainties in this number come from counting statistics.

**Key words:** Galaxies: clusters: luminosity function – galaxies: clusters: individual: Coma – infrared: galaxies

## 1 INTRODUCTION

Recent studies of the optical luminosity function (LF) of galaxies in the Coma cluster (Trentham 1997a; Bernstein et al. 1995; Secker & Harris 1996) have revealed a steep rise at the faint-end, with  $-1.7 < \alpha < -1.3$  for magnitudes fainter than about  $M_R = -15$  (where  $\alpha$  is the logarithmic slope of the LF:  $\phi(L) \propto L^\alpha$ ).

The optical colours and scale-lengths of these faint galaxies suggest that they are probably dwarf spheroidal (dSph, alternatively called dwarf elliptical) galaxies. These galaxies form a distinct family of objects, separate from giant ellipticals on the luminosity – surface-brightness – radius parameter correlations (Kormendy 1987, Binggeli 1994). They have lower surface-brightnesses as their luminosity decreases; well known examples in the Local Group are NGC 205 and Draco. The colour distribution of the

galaxies which produce a steep rise in the LF is heavily peaked at  $B - R = 1.3$ . This is towards the blue end of the range of colours exhibited by local dSphs (Trentham 1997b), but is redder than most of the dwarf irregulars (dIrrs). We cannot distinguish between the two types of galaxies based on their morphologies because (i) they have similar scale-lengths as a function of luminosity (Binggeli 1994), and (ii) these scale-lengths are comparable to the seeing for galaxies in the Coma, so we cannot probe fine details in the structure.

Here, we extend these studies to the near-infrared wavelengths. The  $K$ -band measurements probe the old stellar populations in galaxies as opposed to the younger population probed by the optical wavebands. The aim of this study is two fold: 1). to measure the near-infrared LF of galaxies in Coma and ascertain whether or not the steep rise found at optical wavelengths is seen in the  $K$ -band, and 2). to study

arXiv:astro-ph/9708226v1 25 Aug 1997

the nature of galaxies which dominate the faint-end of the LF (ie. dwarfs), using their optical-infrared colours.

The measurement of the near-infrared LF is not an easy task because of background contamination. At optical wavelengths, the background counts have been well characterized because CCDs cover substantial areas (e.g. Bernstein et al. 1995). In the near-infrared wavelengths, due to the smaller format of the arrays, such detailed measurements cannot be made. A number of medium-deep and deep surveys (Gardner et al. 1993) have permitted detailed measurements of the mean number counts. However, these measurements do not constrain the distribution of the counts around this mean, from field to field as a function of angular size. We compute this distribution from a combination of optical and  $K$ -band observations, and describe this calculation in detail. This is an important part of this study because the field-to-field variance of the background is the dominant source of uncertainty in the LF.

The positions of the cluster dwarfs on an optical-infrared colour-colour diagram allow us to identify the type of galaxy responsible for the upturn in the optical LF, with somewhat more confidence than using the optical observations alone (see above). The difference in optical-near infrared colours between dSph and dIrr galaxies is much bigger than the difference in optical colours, because the dSphs, unlike the dIrrs, have a substantial fraction of the old stellar populations. The similarity in the optical colours between the bluest dSphs and the reddest dIrrs is normally attributed to recent star formation in the blue dSphs; a plausible physical mechanism for this is given by Silk et al. (1987).

This paper is organized as follows. In Section 2, we describe our observing strategy, the observations and data reduction. Section 3 presents the background counts. The near-ir LF for galaxies in the Coma cluster is studied in Section 4. The nature of the dwarf galaxies in the Coma cluster is explored in section 5, using their optical-infrared colours. Finally, our conclusions are summarised in section 6.

Throughout this paper we assume  $H_0 = 75 \text{ km s}^{-1} \text{ Mpc}^{-1}$  and  $\Omega_0 = 1$ .

## 2 OBSERVATIONS AND DATA REDUCTION

### 2.1 The Near-infrared Observations

The requirement to survey a large area of the Coma cluster to deep levels is prevented by the size and sensitivity of near-infrared detectors. For this study, we wish to cover enough area to get good counting statistics after background subtraction, while going deep enough that we can still find the faintest dwarfs. Our observing strategy reflects these two requirements.

We carried out a survey in two parts. A wide-angle shallow ( $K \sim 19$ ) survey of the Coma cluster core was performed using the  $1024 \times 1024$  HgCdTe detector (QUIRC) at the University of Hawaii 2.2 m Telescope. This was then complemented by a deep survey covering a much smaller area in the core to fainter limits ( $K \sim 21$ ), using the  $256 \times 256$  InSb array IRCAM3 at the UKIRT 3.8 m telescope. The areas we surveyed are shown in Figure 1.

We also surveyed an area around the NGC 4839 galaxy

at both the UH 2.2 m and the UKIRT. This galaxy is at the center of a small group, 41 arcminutes to the southwest of the cluster center, and is perhaps in the process of merging with the Coma cluster. Details of the observations and photometry are discussed in the following sub-sections.

### 2.2 The QUIRC (UH 2.2m) Observations and Data Reduction

The observations here were taken at the f/10 Cassegrain focus of the University of Hawaii 2.2 m telescope on Mauna Kea during the nights of March 11–13 1995. The detector was the QUIRC  $1024 \times 1024$  HgCdTe array (scale  $0.19'' \text{ pixel}^{-1}$ , field of view  $3.2' \times 3.2'$ ).

A total of 41.1 square arcminutes of the cluster core (see Figure 1) and a 9.9 square arcminute region, centered on NGC 4839 ( $\alpha(1950) = 12^{\text{h}}54^{\text{m}}59.0^{\text{s}}$ ,  $\delta(1950) = 27^{\circ}46'3''$ ) were imaged, using the  $K'$  filter (Wainscoat & Cowie 1992). The imaging of the core region was done as a  $3 \times 2$  mosaic of individual fields. Exposure times range from 60 mins to 36 mins for the core fields and the NGC 4839 field respectively. The seeing FWHM varied from  $0.9''$  to  $1.1''$ .

Each of the six core field images and the single NGC 4839 image were constructed from a number of three-minute exposures, taken in sets of six, with sky exposures taken between different sets. These images, each of three-minute exposures, were dark and sky subtracted, flatfielded (dome flats were used), and then registered and coadded. The sky fields were chosen to lie in nearby uncrowded regions, and were dithered and median filtered as sets of six two-minute exposures to remove objects in the fields and cosmic rays. This procedure produced images flat to better than one percent.

Instrumental magnitudes were then computed from observations of several ( $\sim 8$  per night) standard stars from the UKIRT Faint Standards list of Casali & Hawarden (1992) and the photometry was converted to the  $K'$  system of Wainscoat & Cowie (1992), using their relation  $K' - K = 0.22(H - K)$ . The zero-point is accurate to about 3%.

We also took images of one blank sky field (9 square arcminutes, centered on  $\alpha(1950) = 15^{\text{h}}$ ,  $\delta(1950) = 40^{\circ}$ ) for a total integration time of 60 minutes. These images were reduced as above, except that the individual exposures themselves were median filtered to construct a sky image for subtraction (this was possible because there were no bright galaxies present). This field will be used to calculate the background counts in the following section, to correct the cluster galaxies for background contamination.

### 2.3 The IRCAM3 (UKIRT) Observations and Data Reduction

The deep observations here were taken at the 3.8 m United Kingdom Infrared Telescope (UKIRT) on Mauna Kea during the nights of March 29–31 1995, using the IRCAM3  $256 \times 256$  InSb array. (scale  $0.286'' \text{ pixel}^{-1}$ , field of view  $1.2' \times 1.2'$ ).

A total of 1.1 square arcminutes of the cluster core was imaged (see Figure 1) using a  $K$  filter. We chose a region that was devoid of very bright galaxies. This  $K$  filter is slightly different from the  $K'$  filter we used for the QUIRC observations; the magnitude zero-point offsets are given by the

equation in the previous section. We also imaged a similar size region centered on NGC 4839. The mean seeing was  $1.0''$ . The total integration times were 6 hours for each field. These images reach  $K = 20.5$  ( $M_K = -14.3$  for galaxies in the Coma cluster assuming a distance modulus of 34.8 mag. for the Coma). This provides the deepest near-infrared survey of a cluster presently available. Instrumental magnitudes were again computed from observations of the UKIRT Faint Standards.

The observing strategy was similar to that described in Section 2.1.1. Each exposure here was 60 seconds, and there were 27 such exposures per set, covering the area around the center of each field. The flatfield frames were constructed using the median filter of the sky frames. For the purpose of sky subtraction, a sky field was chosen to lay outside the cluster (at about  $4^\circ$ , corresponding to 30 times the core radius). All the exposures of this field were combined to make a single deep image. This deep image will also be used to compute the background number counts in the following sections. It is sufficiently well outside the cluster to be safely used for these purposes.

## 2.4 Optical CCD Observations

The optical measurements of the cluster fields used in the following sections are from the UH 2.2 m *B* and *R*-band survey of Trentham (1997a). The details of the observations and reduction are described in that paper. The observations are based on the Johnson (UBV) – Cousins (RI) magnitude system of Landolt (1992).

The optical images of the  $15^h 40^m$  background fields were taken during service time on the INT 2.5 m telescope on La Palma with a Tektronix  $1024 \times 1024$  CCD. The exposure times were 30 minutes each in *B* and *R*; the data reduction was carried out in an identical way to the UH 2.2 m survey data.

## 2.5 Source Detection and Photometry

Using the reduced near-infrared frames, objects were detected at the  $3\sigma$  level above the background, using the detection algorithm FOCAS (Jarvis & Tyson 1981; Valdes 1982, 1989). Their isophotal magnitudes were then estimated and a surface-brightness dependent technique was developed to correct them to the total magnitudes. The technique is described in detail elsewhere (Trentham 1997c) and here we only give a summary of the main steps:

**a)** We measure the sky rms noise,  $\sigma_{rms}$ , and the FWHM seeing,  $b_{FWHM}$ , for each image. We then simulate galaxies of various apparent magnitudes and exponential scale-lengths, convolve them with a gaussian seeing function of width  $b_{FWHM}$  and add Poisson noise of rms magnitude  $\sigma_{rms}$ . Next, the FOCAS detection algorithm was run on this image, searching for objects larger than one seeing disc with fluxes  $3\sigma_{rms}$  above the sky. For each object detected we measure the isophotal magnitude  $m_I$  and its first-moment light radius  $r_1$ . As the true magnitude  $m$  of each object is known, we compute the function  $m(m_I, r_1)$ , and its uncertainty  $\sigma(m)[m_I, r_1]$  for each image. The uncertainty is estimated by investigating how intrinsically identical galaxies are detected differently, depending on the local noise.

We also determine the faintest magnitude  $m_L$ , at which galaxies with intrinsic magnitudes and scale-lengths equal to those of the local dwarfs, projected to the distance of the Coma, are detected with 100% completeness (the magnitude vs. scale-length relation for dwarfs was computed using the data of Kormendy 1987). This will be the faintest magnitude to which we determine the LF in each image.

**b)** We then run the same detection algorithm on our data and make a catalog of all the objects detected at the  $3\sigma$  level (typically  $21 K'$  mag arcsec $^{-2}$  for the QUIRC images and  $23 K$  mag arcsec $^{-2}$  for the IRCAM3 images) above the sky, measuring their  $m_I$  and  $r_1$  parameters. The FOCAS splitting algorithm, which searches for multiple maxima within a single isophote, is used to identify and separate the merged objects.

**c)** Objects are then classified as “galaxies” or “stars” (see Valdes 1989) based on their morphology relative to that of several reference PSF stars in the field. At faint magnitudes ( $K > 18$ ), these classifications are unreliable because many galaxies have apparent scale lengths smaller than the seeing and so, look like stars. Therefore, we correct for stellar contamination at faint magnitudes by computing the number of faint stars expected, given the number of bright ( $K < 17$ ) stars and assuming some Galactic stellar luminosity function slope (we adopt the slope measured at optical wavelengths by Jones et al. 1991). For the Coma, which lies well out of the Galactic plane, this is a small effect ( $< 5\%$ ) and the uncertainties generated by this method are negligible.

**d)** From our measured  $m_I$  and  $r_1$  values, for each object in our catalog, we then compute  $m$  and its uncertainty  $\sigma(m)$ , bin them in half-magnitude (QUIRC) or one-magnitude (IRCAM3) intervals, and correct for stellar contamination as in (c) above. The number counts (in units of number per magnitude per square degree) are then computed by dividing the number of galaxies in each bin by the area of the survey. The uncertainties in the number counts is the quadrature sum of counting statistics and uncertainties from the isophotal corrections  $\sigma(m)$ . This surveyed area includes a correction for crowding, the process by which faint galaxies go undetected because they happen to fall within the detection isophote of a much brighter object.

For each object, we also compute the aperture magnitude  $m_a$  within an aperture diameter of  $3.0''$ . The colours of the faint objects are measured by taking the difference between their aperture magnitudes in different bands. Isophotal magnitudes are not used for computing colours because the detection isophotes are not the same in different bands. The selected aperture here is large enough that differential seeing effects between different images are negligible. This method fails to give accurate colours for bright galaxies if colour gradients are large. However, in this study only colours for the fainter galaxies ( $K > 15.5$ ) will be explored.

The *K*-band Galactic extinction is negligible for both the cluster and background fields here (based on their positions in the HI maps of Burstein & Heiles 1982) and hence, has been ignored in this investigation. The above technique was applied to both our cluster and background fields. The total magnitudes and colours for galaxies detected in both the QUIRC and IRCAM3 surveys were then estimated.

### 3 THE K-BAND NUMBER COUNTS

In this study, we surveyed two background fields, one with QUIRC (the 15<sup>h</sup> 40<sup>o</sup> field – see Section 2.1.1), and one with IRCAM3 (the sky field 4<sup>o</sup> outside the Coma core – see Section 2.1.2). In Figure 2, we present the background number counts for our fields, compared with the number counts from the literature as compiled by Gardner et al. (1993). Here, all the photometry is converted to the *K* system, to ensure internal consistency. Our data agrees well with that of previous studies, but our errors are larger. The dashed line represents the mean number counts, computed using *all* the data in Figure 2. The number counts corresponding to this line will be used to correct the counts in the Coma cluster for background contamination.

The uncertainty in using the mean value of  $\Delta N(K)$  for a field size probed by our survey (i.e. the field-to-field variance in the background counts) must be quantified, as this will be a major source of uncertainty in the LF. This has not been measured directly in the *K*-band, because of the small size of the arrays. It has, however, been measured at optical wavelengths (see Bernstein et al. 1995 and Trentham 1997c for an estimate of  $\Delta N(R)$  and  $\Delta N(B)$ ). Also, the distribution of *B* – *K* colours for galaxies as a function of *K* has been measured (Gardner et al. 1993). We therefore estimate, for fields having the same area,

$$\Delta N(K) = N(K) \frac{\int_B \left(\frac{\Delta N}{N}\right)_B f(B-K) dB}{\int_B f(B-K) dB}, \quad (1)$$

where  $f(B-K)$  is the distribution of *B* – *K* colours for a given *K*. We approximate  $f(B-K)$  to a gaussian with the mean value given by Gardner et al. (1993)– (see their Fig. 3), and a standard deviation of 1 magnitude. The values of  $\left(\frac{\Delta N}{N}\right)_B$  are taken from Trentham (1997c).

We now calculate  $\Delta N(K)$  from Equation 1, correcting for different area sizes, using Poisson statistics (Figure 3). For the Coma core field, this correction is small, since the total field size of our mosaic is comparable to the field size used to derive  $\Delta N$  at optical wavelengths.

### 4 THE NEAR-INFRARED LUMINOSITY FUNCTION IN THE COMA CLUSTER

The number of galaxies detected in each *K* magnitude bin in the Coma cluster are estimated for both the QUIRC (Table 1) and IRCAM3 (Table 2) observations. The fields have different magnitude limits because the seeing and exposure time varied. This is the reason why the numbers of fields in the last rows of Table 1 (core section) are smaller than in the other rows. The *K*-band number counts for galaxies in the Coma cluster are shown in Figure 4, along with the mean background line described in the previous section.

The luminosity function is computed by subtracting the background contribution from the cluster number counts. The associated uncertainty in the LF takes into account both the field-to-field variance in the background, as shown in Figure 3, and the errors described in Section 2.3 and shown in Figure 4.

The near-infrared LF for the Coma core field is presented in the upper panel of Figure 5 (a distance modulus

of 34.8 mag. is assumed for the Coma cluster). After subtracting the background contribution, some of the magnitude bins are left with no galaxies (i.e. negative number in that bin) and therefore, on this logarithmic plot, only the upper errorbars are shown. The most obvious feature of the LF is its poor statistics. The errors are the quadrature sums of the uncertainties from counting statistics, measurements of the total magnitudes, and the field-to-field variance of the background. At the faintest magnitudes, uncertainties due to background contamination dominates (so, changing the binning will not help). This problem will remain until it is possible to image much greater areas of the cluster to fainter limits. The implication here is that a well-constrained measurement of the *K*-band LF for dwarf galaxies in Coma is not feasible at present, at least if this is carried out by performing a simple background subtraction. Morphological information does not help since the apparent scale-lengths of the Coma dwarfs are similar to those of background late-type galaxies, and are close to the seeing disk. A more instructive approach might be to make a background subtraction, taking into account the colours of galaxies. This requires detailed measurement of the field-to-field variance of the background counts as a function of colour (concentrating on colours similar to those of the cluster galaxies). This is not a trivial measurement, but is easier than the wide-field surveys of clusters to faint magnitudes described above. However, the variance cannot be estimated, using a strategy similar to that outlined in Section 3, because the contribution to  $\left(\frac{\Delta N}{N}\right)_B$ , by galaxies of different colours, is not known.

The shape of the *K*-band LF, within the errors, is roughly consistent with that of the optical (*R*-band, shifted by about 3 magnitudes) LF for the Coma core field. The IRCAM3 observations, which probe a magnitude range where the optical LF is steeply increasing, are systematically higher than the QUIRC points but this, in part, could also be a normalization effect (the IRCAM3 and QUIRC surveys covered different areas). The large error bars mean that the parameters from any fit to our *K*-band data will be poorly constrained. A Schechter (1976) function fit to the QUIRC data, where we fix  $M_K^* = -24.35$  (Barger et al. 1996) gives

$$\alpha^* = -1.10, \log_{10} N^* = 2.49, \nu = 18, \frac{\chi^2}{\nu} = 0.58.$$

Alternatively, a power-law fit for the range  $-20.3 < M_K < -16.3$  gives  $\alpha = -0.83_{-0.99}^{+1.83}$ .

For the NGC 4839 field, the problems of large uncertainties due to background subtraction are worse because of the smaller field size and hence, a lower galaxy density. The *K*-band LF in this region is essentially unconstrained.

Finally, we stress that in spite of the above difficulties, Coma is still the best cluster for measuring the *K*-band LF of dwarf galaxies. For more distant, but richer clusters like Abell 665 ( $z = 0.2$ ), we have many more cluster galaxies relative to the background and hence, the LF is less sensitive to  $\Delta(N)$ . However, we cannot realistically probe the faintest magnitudes in these clusters (where the dwarfs are numerous). For more nearby clusters like the Virgo, we can probe the faintest absolute magnitudes, but then covering an area large enough that counting statistics are reasonable is difficult, considering the field of view of the near-infrared array detectors.

## 5 THE OPTICAL-IRRED COLOURS OF DWARFS IN FIELD AND CLUSTERS

The  $B - K$  vs.  $B - R$  colour-colour diagram for the QUIRC data is shown in Figure 6. The objects with  $B - K > 5$  are expected to be background late-type galaxies. Most of the galaxies in the  $15^{\text{h}} 40^{\circ}$  field, and many of the galaxies in the Coma core field reside in this part of the diagram.

The cluster galaxies are most likely the condensation seen in the figure with  $1.2 < B - R < 1.6$ , based on their optical colours (Trentham 1997a). These galaxies have  $B - K$  colours somewhat redder than that of the dIrr galaxies at any  $z$ . This confirms our conclusion from the optical observations, that the faint galaxies in the Coma are dSphs. A histogram of the  $B - K$  colours of galaxies with  $1.2 < B - R < 1.6$  is presented in Figure 7. This histogram extends from  $B - K = 3$  to  $B - K = 5$ , peaking at  $B - K = 3.6$ . The vertical error bars in this figure are the  $\sqrt{N}$  counting errors and are large enough that conclusions about the detailed shape of the histogram cannot be made. Nevertheless, the  $B - K$  colour distribution seems broader than the  $B - R$  distribution (Trentham 1997a). This observation can be explained if the dSphs in the Coma cluster have a more homogeneous history regarding their most recent star formation burst (which is probed by the  $B - R$  colour) compared to their integrated star formation history (which is probed by the  $B - K$  colour). Such a scenario is expected if the Coma cluster is a merger between two smaller clusters (as suggested by its lack of a cooling flow and its two brightest cluster galaxies) and if star formation was induced in most of the low mass galaxies at this time (see Silk et al. 1987).

The absence of background galaxies in the part of the colour-colour diagram where the cluster dwarfs reside is encouraging. This confirms our conclusion in Section 4 that using colour information to make a background subtraction (to measure the  $K$ -band cluster LF) may well be feasible. Such a strategy requires an extension of the measurements presented in Figure 6 to a larger magnitude range to improve the background statistics by observing a number of background fields in 3 colours. For each magnitude bin, a plot identical to Figure 6 can be constructed and used to perform the background subtraction based on a local “density on the  $B - K$  vs.  $B - R$  plane” criterion. The field-to-field variance would probably still be large, but the fractional contamination of the background will be lower, so the LF would be much better constrained.

This prescription is implemented and the results presented in Figure 8, where the LF for all the galaxies with  $B - K < 5$  and  $1.2 < B - R < 1.6$  in Figure 7 is shown. There are no galaxies in the  $15^{\text{h}} 40^{\circ}$  background field in this part of the  $B - K$  vs.  $B - R$  plane, and we assume zero background contamination in our cluster fields. Only counting statistics are used in deriving the uncertainties. The estimated LF here is still not well constrained; a power-law fit to the data gives  $\alpha = -1.41_{-0.37}^{+0.34}$ . This is close to the values measured by Secker & Harris (1996) and Trentham (1997a) for this part of the LF (assuming  $R - K \approx 3$ ), but the errors are still large, and are likely to be underestimates. The errors must increase as we take the background into account. A more accurate estimate of the uncertainties here needs more wide-field optical/near-infrared surveys and hence, a

characterisation of the background variance, as described in Section 4. Also, the cluster members that do not lie in this part of the  $B - K$  vs.  $B - R$  plane are missed, introducing a selection effect. However, with a few times the area of this survey, the counting errors become manageable, and if the background contamination really is small, a measurement of the  $K$ -band LF seems feasible. Such a survey will be possible shortly, when larger infrared arrays become available.

## 6 CONCLUSIONS

A  $K$ -band survey of the Coma cluster has been carried out. This consists of a wide-angle shallow ( $K \sim 19$ ) survey with the QUIRC (UH 2.2m) and a deeper survey ( $K \sim 21$ ), covering a much smaller area with the IRCAM3 (UKIRT). These observations were used to construct the near-infrared LF of galaxies in the Coma cluster and to study the nature of the population dominating the faint-end of the LF. The results of this study are summarised as follows:

- (i) The  $K$ -band LF in the Coma cluster is not well constrained. However, within the estimated (large) errors, this is consistent with the  $R$ -band LF, shifted by  $\sim 3$  magnitudes.
- (ii) The optical-infrared colours of these faint galaxies confirm that they are dwarf spheroidals. The median  $B - K$  colour for galaxies with  $-19.3 < M_K < -16.3$  is 3.6 mag.
- (iii) Using the  $B - K$  vs.  $B - R$  colour-colour diagram, a region on this plane is identified where the background galaxies are rare ( $B - K < 5$ ;  $1.2 < B - R < 1.6$ ). It is proposed that a more accurate measurement of the  $K$ -band LF for clusters can be carried out if the background contamination is estimated as a function of colour.
- (iv) Using the  $B - K$  and  $B - R$  colours to correct the Coma cluster data for background contamination (as in 3 above), the  $K$ -band LF is again constructed. The logarithmic slope of the LF in the range  $-19.3 < M_K < -16.3$  mag. is  $\alpha = -1.41_{-0.37}^{+0.34}$ .

## REFERENCES

- Barger A. J., Aragon-Salamanca A., Ellis R. S., Couch W. J., Smail I., Sharples R. M., 1996, MNRAS, 279, 1
- Bernstein G. M., Nichol R. C., Tyson J. A., Ulmer M. P., Wittman D., 1995, AJ,
- Binggeli B., 1994, in Meylan G., Prugneil P., ed., ESO Conference and Workshop Proceedings No. 49: Dwarf Galaxies. European Space Observatory, Munich, p. 13
- Burstein D., Heiles C., 1982, AJ, 87, 1165
- Casali M. M., Hawarden T. G., 1992, The JCMT-UKIRT Newsletter Vol. 4, p. 33
- Coleman G. D., Wu C.-C., Weedman D. W., 1980, ApJS, 43, 393
- Cowie L. L., Gardner J. P., Hu E. M., Songaila A., Hodapp K. W., Wainscoat R. J., 1994, ApJ, 434, 114
- Gardner J. P., 1992, PhD Thesis, University of Hawaii
- Gardner J. P., Cowie L. L., Wainscoat R. J., 1993, ApJ, 415, L9
- Glazebrook K., Peacock J. A., Collins C. A., Miller L., 1994, MNRAS, 266, 65
- Huang J. S., Cowie L. L., Gardner J. P., Hu E. M., Songaila A., Wainscoat R. J., 1997, ApJ, in press
- Kormendy J., 1987, in Faber S. M. ed., Nearly Normal Galaxies. Springer-Verlag, New York, p. 163
- Landolt A. U., 1992, AJ, 104, 340
- Jarvis J. F., Tyson J. A., 1981, AJ, 86, 476

- Jones L. R., Fong R., Shanks T., Ellis R. S., Peterson B. A., 1991, *Schechter P.*, 1976, *ApJ*, 203, 297  
 Secker J., Harris W. E., 1996, *ApJ*, 469, 623  
 Silk J., Wyse R. F. G., Shields G. A., 1987, *ApJ*, 322, L59  
 Trentham N., 1997a, *MNRAS*, submitted  
 Trentham N., 1997b, *MNRAS*, submitted  
 Trentham N., 1997c, *MNRAS*, in press  
 Valdes F., 1982, *Proc. SPIE*, 331, 465  
 Valdes F., 1989, in Grosbol P. J., Murtagh F., Warmels R. H., ed., *ESO Conference and Workshop Proceedings No. 31: Proceedings of the 1st ESO/St-ECF Data Analysis Workshop*. European Space Observatory, Munich, p. 35  
 Wainscoat R. J., Cowie L. L., 1992, *AJ*, 103, 332

## 7 FIGURE CAPTIONS

**Figure 1:** The Palomar Sky Survey image of the core of the Coma cluster. The image is 11.2 arcminutes square; north is up and east is to the left. The black (UH 2.2 m) and white (UKIRT) boxes outline the regions covered by this survey. The two bright central galaxies are NGC 4874 ( $\alpha(1950) = 12^{\text{h}}57^{\text{m}}11.0^{\text{s}}$ ,  $\delta(1950) = 28^{\circ}13'46''$ ) and NGC 4889 ( $\alpha(1950) = 12^{\text{h}}57^{\text{m}}43.3^{\text{s}}$ ,  $\delta(1950) = 27^{\circ}46'3''$ ).

**Figure 2:** The magnitude – number count relation for the  $K$ -band. The solid symbols represent the data from this study (one QUIRC field, and one IRCAM3 field, as described in the text). The  $K$ -band magnitudes are used. The QUIRC data have been corrected to this system assuming  $H - K = 0.5$  for typical field galaxies and  $K' - K = 0.22(H - K)$ . The open symbols refer to the counts from a number of studies, taken from the compilation of Gardner et al. (1993, see also Gardner 1992). The abbreviations in the key are HDS = Hawaii Deep Survey (see also Cowie et al. 1994); HMDS = Hawaii Medium Deep Survey; HWDS = Hawaii Medium Wide Survey; GPCM = Glazebrook et al. 1994; HWS = Hawaii Wide Survey. The dashed line shows the mean value of  $N$  in  $K$  magnitude bins, computed from all the data presented here.

**Figure 3:** The field-to-field variance in the background for the  $K$ -band, computed as described in the text. The kink at  $K \sim 17$  corresponds to the discontinuity in the mean value of  $f(B - K)$  (see Figure 3 of Gardner et al. 1993).

**Figure 4:** The magnitude – number count relation for our Coma core (upper panel) and NGC 4839 field (lower panel) data, computed as described in the text. The magnitudes here are  $K'$  for the QUIRC data and  $K$  for the UKIRT data. The dashed line represents the mean  $K'$ -band number counts as a function of magnitude, computed from the equivalent  $K$ -band line in Figure 2, assuming  $K' - K = 0.22(H - K)$  for a typical field galaxy.

**Figure 5:** The  $K$ -band luminosity function of the Coma core (upper panel) and NGC 4839 group (lower panel). The  $R$ -band data is from Trentham (1997a) and has been normalized to minimize the scatter between  $N(K)$  and  $N(R + 3)$ . The magnitude system is  $K'$  for the QUIRC data and  $K$  for the UKIRT data (last two points only in the upper panel and last point only in the lower panel). We do not correct all the data to a single magnitude system because of

our lack of knowledge of  $H - K$  for the cluster dwarfs. Slopes corresponding to two values of  $\alpha$  are shown. We assume a distance modulus of 34.8. After subtracting the background contribution, some magnitude bins are left with no galaxies. These are indicated by their upper errorbars (with no mean points) only.

**Figure 6:** The  $B - K$  vs.  $B - R$  colour-colour diagram for galaxies having  $15.5 < K < 18.5$ . Aperture magnitudes (diameter  $d = 3.0''$ ) are used in computing the colours. All our data are from the QUIRC images, using the  $K'$  magnitudes. Only objects classified by FOCAS as galaxies in all three images are included.

Different lines represent the colour–colour relations for different types of galaxies. The redshift varies along the paths shown in the diagram, from 0 (at the bottom left extremity of each path) to the number shown in parentheses in the legend. The optical  $K$ -corrections are from Coleman et al. (1980) for the giant and dIrr galaxies and from Trentham (1997b) for the dSph galaxies. The  $K$ -band  $K$ -corrections come from Huang et al. (1997). The position in this colour-colour diagram of a giant elliptical at the redshift of Coma is marked by X. We estimate uncertainties corresponding to 0.1 and 0.15 mag. in  $B - R$  and  $B - K$  colours respectively.

**Figure 7:** The  $B - K$  histogram of galaxies in the Coma core field with  $1.2 < B - R < 1.6$ . These are the galaxies which, based on their optical colours, are most likely to be cluster members, and have magnitudes faint enough to be in the part of the LF that is steeply rising.

The background contamination is small. Only three galaxies in the  $15^{\text{h}} 40^{\text{m}}$  background field (this has an area of about 20% of the Coma core field) satisfy the requirements for inclusion here. There have  $B - K$  of 5.14, 5.53, and 5.99.

**Figure 8:** The luminosity function of the galaxies shown in Figure 7 with  $B - K < 5$ , assuming no background contamination. As in Figures 6 and 7,  $d = 3.0''$  aperture magnitudes are used; for these faint galaxies. This is a good approximation to the total magnitudes.

This figure "fig1.jpg" is available in "jpg" format from:

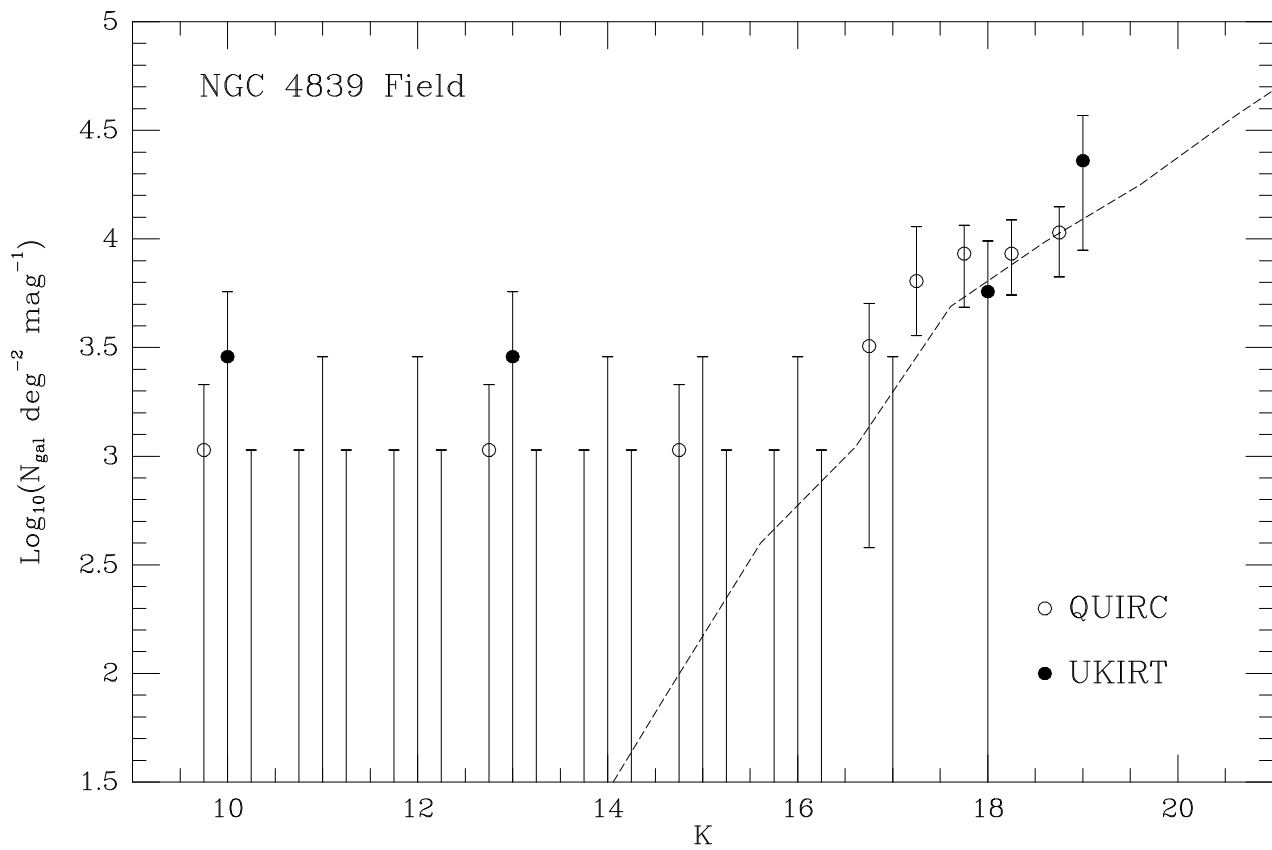
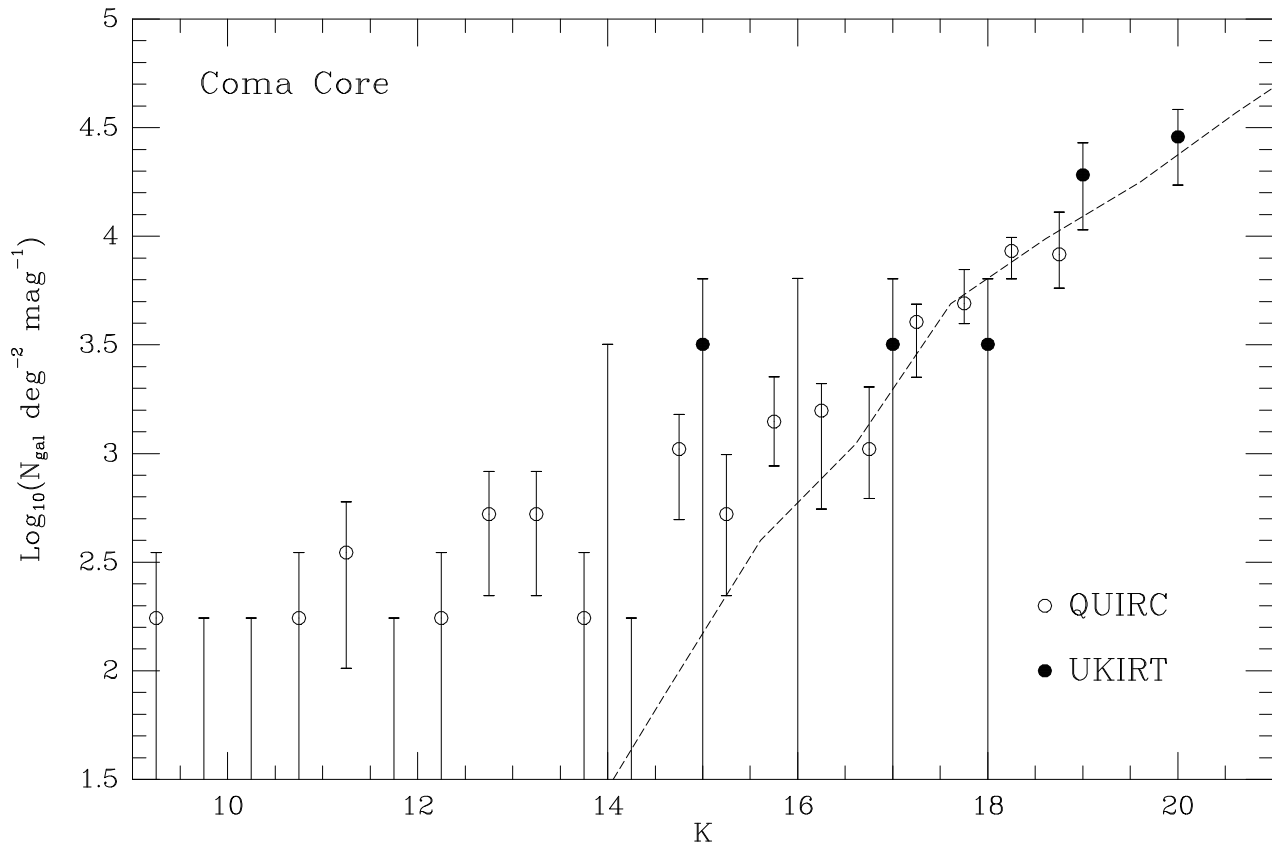
<http://arxiv.org/ps/astro-ph/9708226v1>

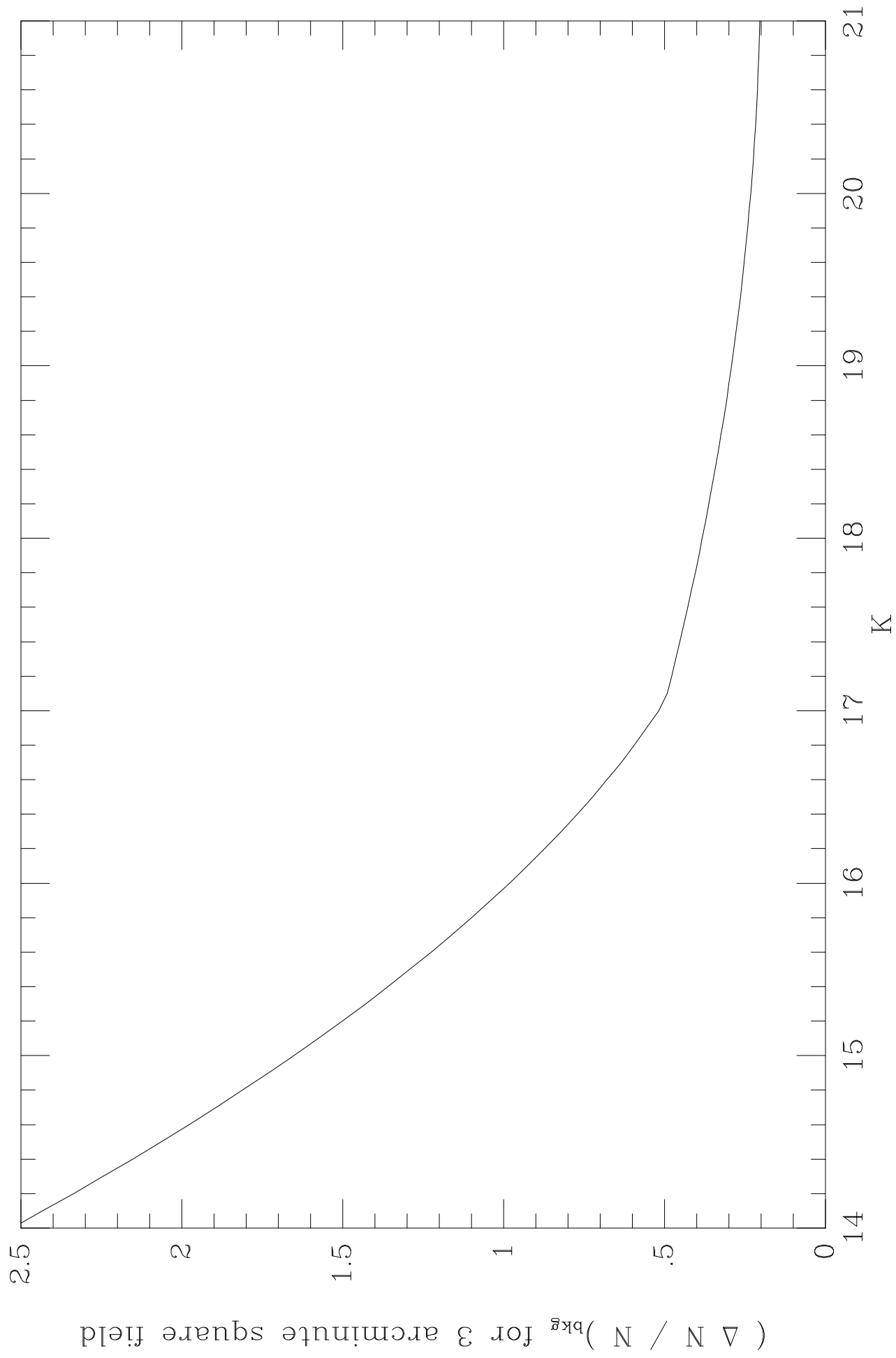


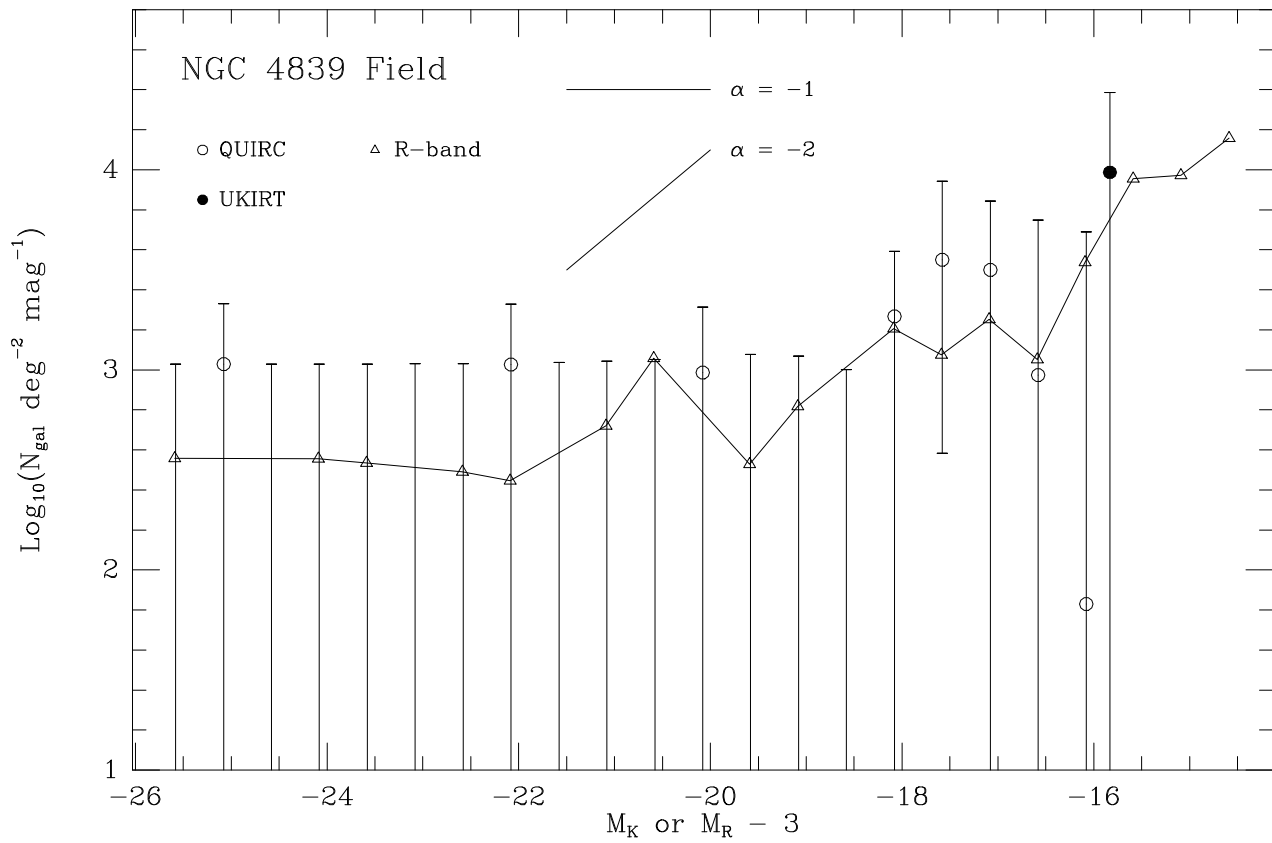
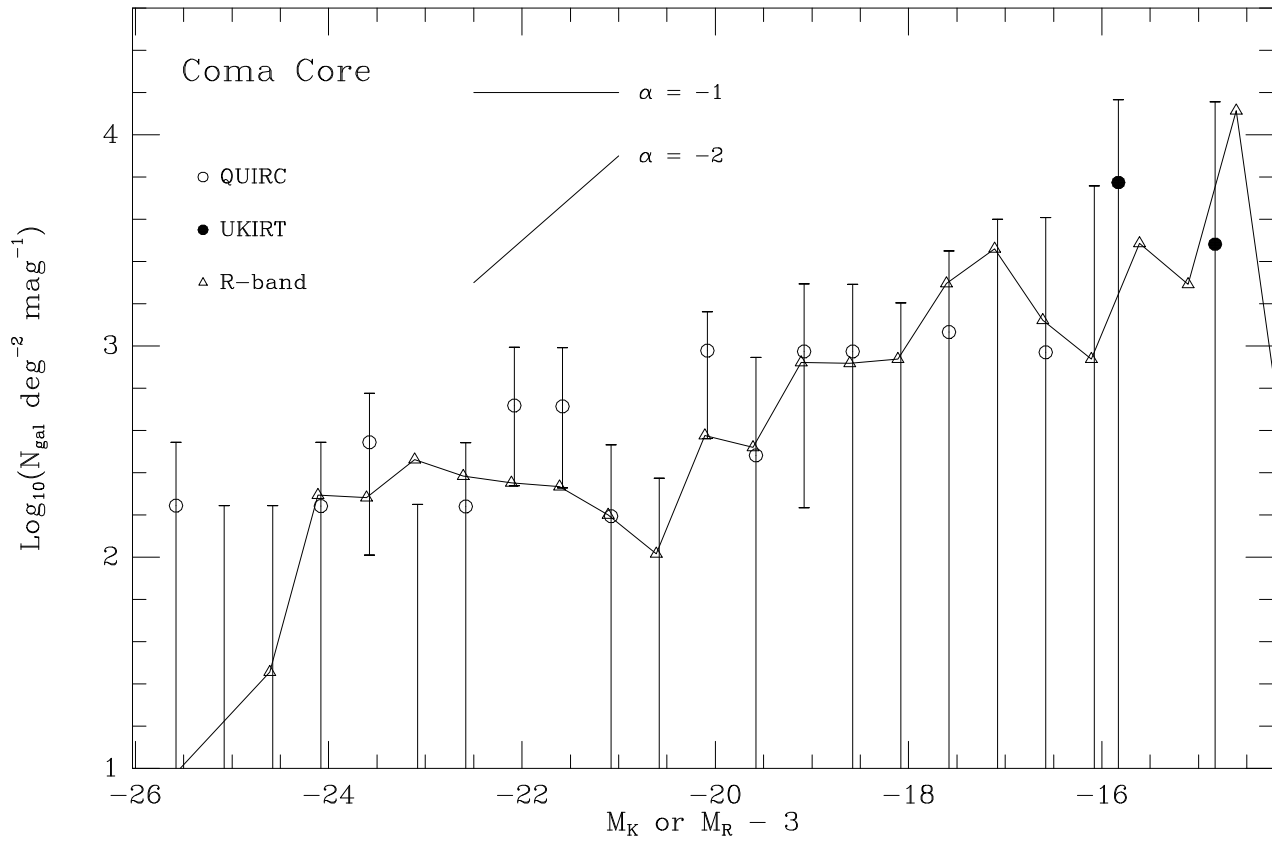


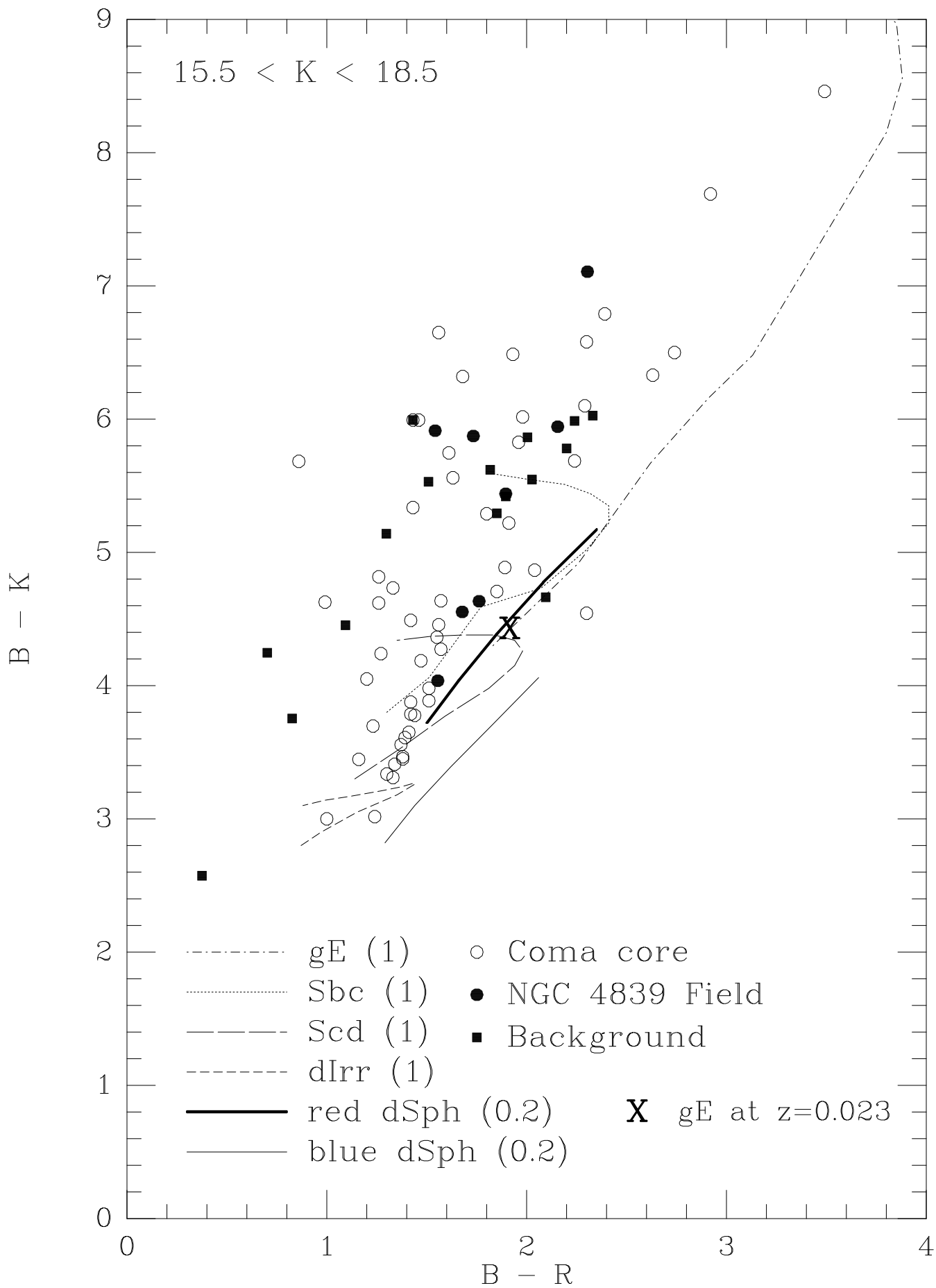
**Table 2**  
**UKIRT observations**

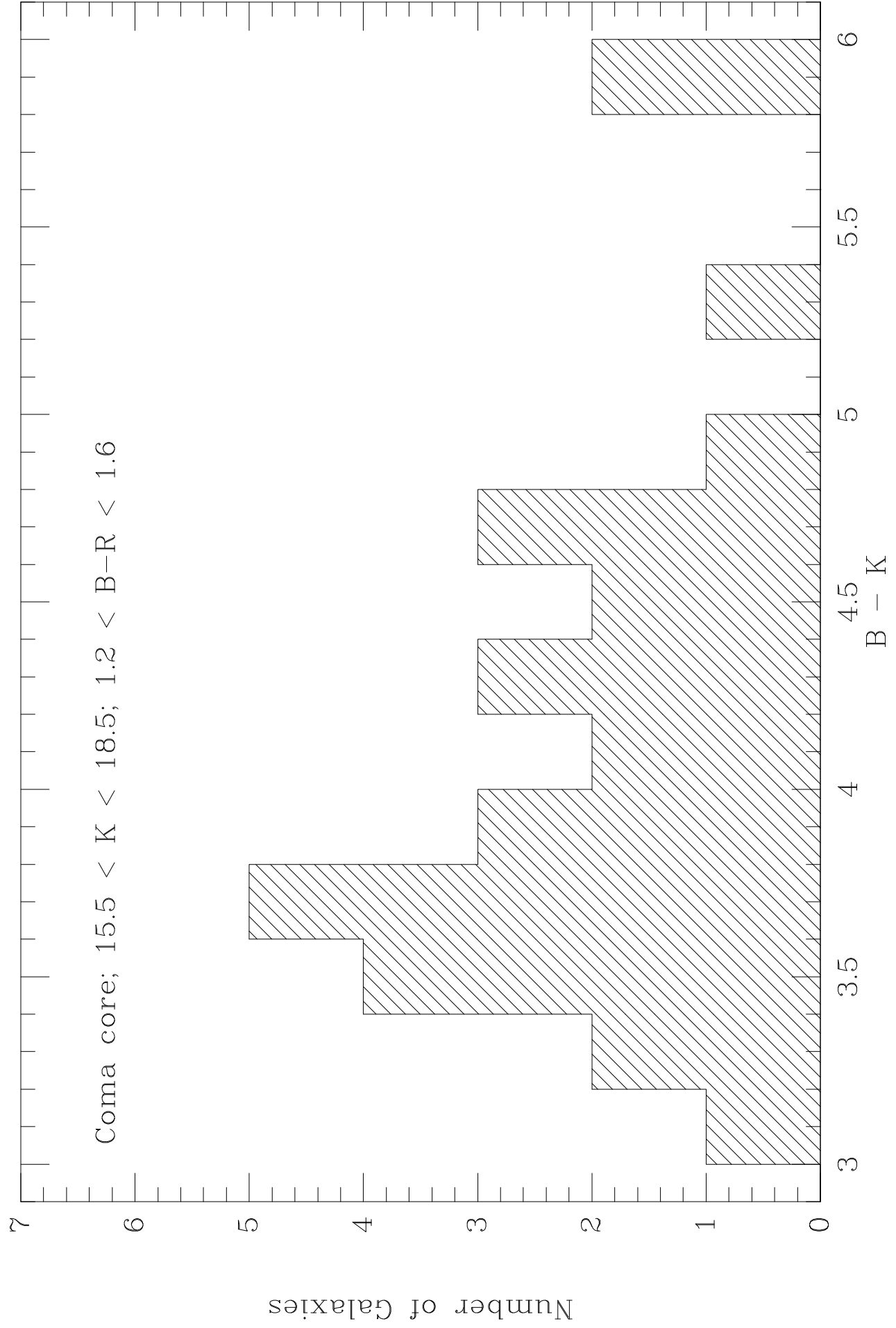
$K$	$N_{\text{gal}}$	$N_{\text{bkg}}$	$\left(\frac{\Delta N}{N}\right)_{\text{bkg}}$
	Measured	Predicted (Fig. 2)	Predicted (Fig. 3)
<b>Coma core</b>			
14.0	0	0.0	7.2
15.0	$1 \pm 1$	0.1	4.7
16.0	0	0.2	2.8
17.0	$1 \pm 1$	0.7	1.5
18.0	$1 \pm 1$	2.1	1.1
19.0	$7^{+2.6}_{-2.8}$	4.0	0.83
20.0	$9^{+3.6}_{-3.0}$	7.8	0.66
<b>NGC 4839 Field</b>			
9.0	0	0.0	—
10.0	$1 \pm 1$	0.0	—
11.0	0	0.0	—
12.0	0	0.0	—
13.0	$1 \pm 1$	0.0	—
14.0	0	0.0	7.0
15.0	0	0.1	4.6
16.0	0	0.2	2.7
17.0	$0^{+1.4}_{-0.0}$	0.8	1.4
18.0	$2^{+1.4}_{-2.0}$	2.2	1.1
19.0	$8^{+4.9}_{-4.9}$	4.3	0.81











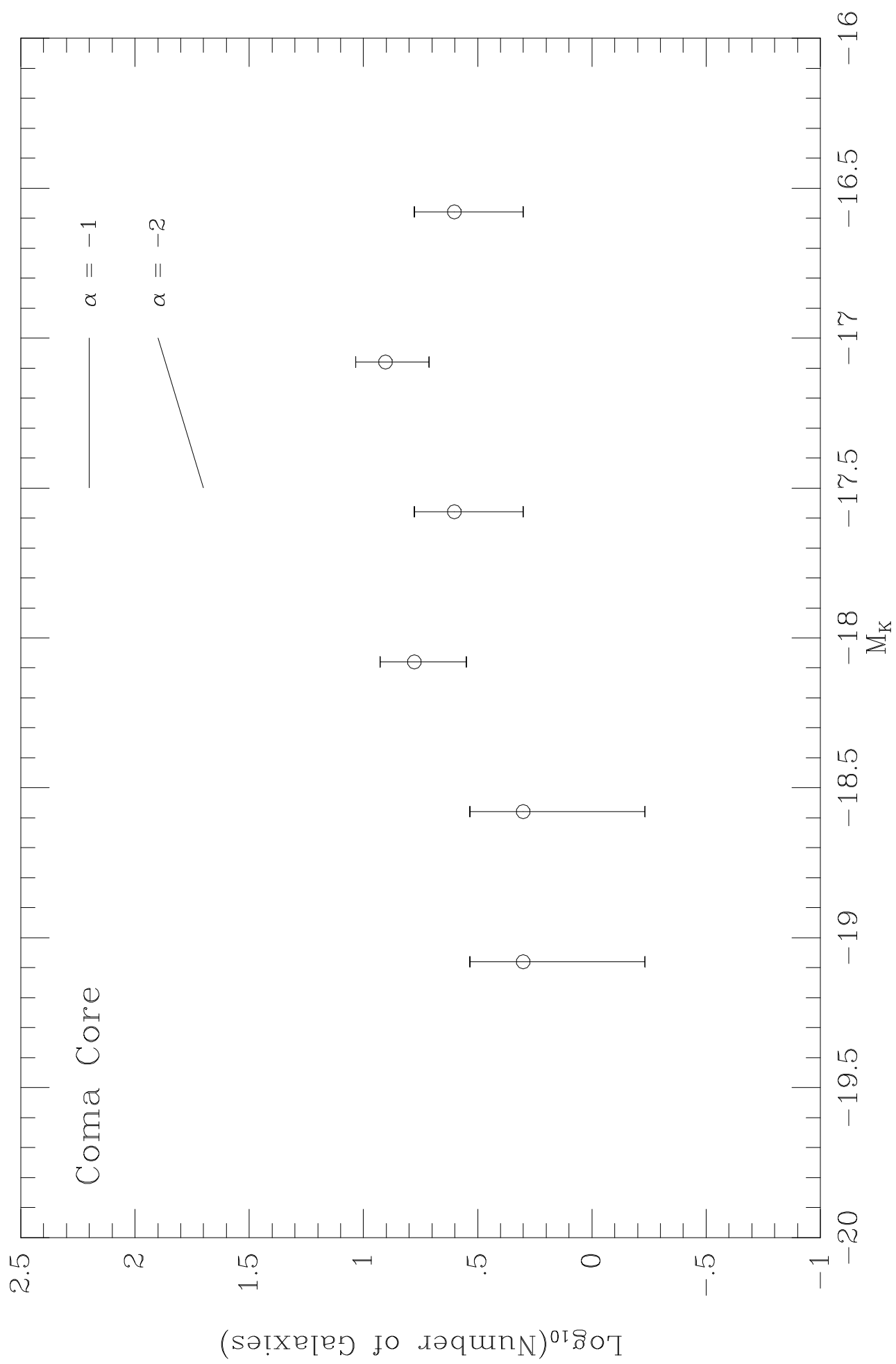


**Table 1**  
**QUIRC observations**

$K'$	Number of Fields	$N_{\text{gal}}$	$N_{\text{bkg}}$	$(\frac{\Delta N}{N})_{\text{bkg}}$
		Measured	Predicted (Fig. 2)	Predicted (Fig. 3)
<b>Coma core</b>				
9.25	6	$1 \pm 1$	0.0	—
9.75	6	0	0.0	—
10.25	6	0	0.0	—
10.75	6	$1 \pm 1$	0.0	—
11.25	6	$2 \pm 1.4$	0.0	—
11.75	6	0	0.0	—
12.25	6	$1 \pm 1$	0.0	—
12.75	6	$3 \pm 1.7$	0.0	—
13.25	6	$3 \pm 1.7$	0.0	1.6
13.75	6	$1 \pm 1$	0.1	1.4
14.25	6	0	0.2	1.1
14.75	6	$10^{+2.6}_{-3.2}$	0.6	0.92
15.25	6	$3^{+2.6}_{-1.7}$	1.3	0.73
15.75	6	$8^{+4.9}_{-3.0}$	2.6	0.57
16.25	6	$9^{+3.0}_{-5.8}$	4.4	0.45
16.75	6	$6^{+5.6}_{-2.4}$	7.8	0.32
17.25	6	$23^{+4.8}_{-10.2}$	16.3	0.23
17.75	6	$28^{+12.2}_{-5.4}$	30.7	0.20
18.25	5	$40^{+6.3}_{-10.2}$	35.6	0.19
18.75	3	$23^{+12.9}_{-6.9}$	29.6	0.22



**Table 1 continued**

$K'$	Number of Fields	$N_{\text{gal}}$	$N_{\text{bkg}}$	$(\frac{\Delta N}{N})_{\text{bkg}}$
		Measured	Predicted (Fig. 2)	Predicted (Fig. 3)
<b>NGC 4839 Field</b>				
9.25	1	0	0.0	—
9.75	1	$1 \pm 1$	0.0	—
10.25	1	0	0.0	—
10.75	1	0	0.0	—
11.25	1	0	0.0	—
11.75	1	0	0.0	—
12.25	1	0	0.0	—
12.75	1	$1 \pm 1$	0.0	—
13.25	1	0	0.0	—
13.75	1	0	0.0	—
14.25	1	0	0.0	2.8
14.75	1	$1 \pm 1$	0.1	2.3
15.25	1	0	0.2	1.8
15.75	1	0	0.4	1.4
16.25	1	$0^{+1.4}_{-0.0}$	0.7	1.1
16.75	1	$3^{+1.7}_{-2.6}$	1.3	0.79
17.25	1	$5^{+5.4}_{-2.2}$	2.7	0.58
17.75	1	$8^{+2.8}_{-3.5}$	5.0	0.50
18.25	1	$8^{+3.5}_{-2.8}$	7.1	0.43
18.75	1	$10^{+3.2}_{-4.4}$	9.9	0.38